

# Reliability Assessment of Laminated Composite Plates with Random Strength Parameters

T. Y. Kam,\* K. H. Chu,† and E. S. Chang†

National Chiao Tung University, Hsin-Chu 300, Taiwan, Republic of China

A method is presented for the reliability assessment of transversely loaded laminated composite plates with random strength parameters. The proposed method is constructed on the basis of the first-ply failure method and the series system hypothesis. The first-ply failure analysis of a laminated plate is achieved via the use of a phenomenological failure criterion and the finite element method. In the reliability analysis, the independent (maximum stress) as well as the dependent (Tsai-Hill) failure criteria are used to establish the limit state equation; a direct numerical integration method together with the series system hypothesis are adopted to compute the reliability of the plate. Experimental investigations of lamina strength distributions and first-ply failure of laminated composite plates were performed. It has been found that lamina strengths and first-ply failure load can be well fitted by Weibull distributions. The baseline probability distributions of lamina strength parameters determined from the tests are then used in the reliability analysis of the laminated composite plates. The accuracy of the proposed method in reliability prediction of the laminated composite plates of different sizes is verified against the experimental results.

## Introduction

LAMINATED composite plates or panels are commonly used in the construction of weight-sensitive structures such as aircraft, automobile, mechanical, and marine structures. In general, these structures are operated in severe environments and require high reliability. To ensure that no sudden catastrophe of a structure may occur during its lifetime, the reliability of the structure must be thoroughly investigated in the development stage. To have an effective and meaningful reliability assessment, the reliability analysis of laminated composite structures has thus become an important subject of research. Recently, a number of researchers have studied the reliability of laminated composite members. For instance, Cederbaum et al.,<sup>1</sup> Cederbaum and Aboudi,<sup>2</sup> and Sun and Yamada<sup>3</sup> studied the reliability of composite laminates subjected to in-plane loads. Cassenti<sup>4</sup> presented a method for evaluating the failure probability of laminated composite beams and plates subjected to flexural bending. Gurvich and Pipes<sup>5</sup> presented a multistep failure probabilistic model for the reliability analysis of laminated composite beams under bending. Kam and Lin,<sup>6</sup> Kam et al.,<sup>7</sup> and Engelstad and Reddy<sup>8</sup> studied the reliability of linear or nonlinear laminated composite plates subjected to transverse loads. The previous reliability studies of laminated composite members, however, have been concentrated on the theoretical aspect, and only limited experimental data were presented to verify the accuracy of their proposed methods.

In this paper, the reliability of laminated composite plates with random strength parameters subjected to transverse loads is studied. The limit state equation of the laminated composite plates is constructed on the basis of the maximum stress or Tsai-Hill failure criteria. A direct numerical integration technique together with the series system hypothesis are used to evaluate the reliability of the laminated composite plates. Experiments were conducted to investigate the probability distributions of strength parameters and first-ply failure loads of laminated composite plates. The accuracy of the proposed method is verified against the experimental data.

## First-Ply Failure Analysis

The first-ply failure analysis of a laminated composite plate is accomplished using the finite element method and an appropriate

phenomenological failure criterion. The finite element is constructed on the basis of the first-order shear deformation theory and contains five degrees of freedom (three displacements and two shear rotations) per node.<sup>9</sup> In the evaluation of the element stiffness matrix, a nine-node Lagrangian element with reduced integration using a  $2 \times 2$  Gauss rule is adopted. Stresses at the nodes of an element are determined from those at the integration points by extrapolation. Five independent stress components at any point in the plate are considered in the finite element analysis. The failure analysis of the laminated plate is performed in turn using an independent or a dependent failure criteria.<sup>10</sup> The independent failure criterion adopted in the failure analysis is maximum stress criterion that states that the ratios of stresses in the principal material directions to the respective strengths must be less than 1, otherwise failure is said to have occurred; that is,

$$R_i = \sigma_i / X_i < 1 \quad (i = 1, 2, 4, 5, 6) \quad (1)$$

where  $R_i$  are stress ratios;  $\sigma_1$  and  $\sigma_2$  are normal stress components;  $\sigma_4$ ,  $\sigma_5$ , and  $\sigma_6$  are shear stress components;  $X_1$  and  $X_2$  are the lamina normal strengths in the 1 and 2 directions; and  $X_4$ ,  $X_5$ , and  $X_6$  are the shear strengths in the 23, 13, and 12 planes, respectively. When  $\sigma_1$  and  $\sigma_2$  are of a compressive nature, they should be compared with  $X_{1C}$  and  $X_{2C}$ , which are normal strengths in compression along the 1 and 2 directions, respectively. In the deterministic first-ply failure analysis of laminated composite plates, stress ratios in the constituent plies at the integration points, as well as the nodes of the elements, are determined, and the largest stress ratio is used to check if failure has occurred. The advantage of using the maximum stress criterion in the failure analysis is that the dominant failure mode can be easily identified. Based on the present finite element method, one of the following failure modes is likely to occur: fiber breakage ( $\sigma_1 > X_1$ ), matrix tensile fracture ( $\sigma_2 > X_2$ ), in-plane shear failure ( $\sigma_6 > X_6$ ), fiber direction transverse shear failure ( $\sigma_5 > X_5$ ), matrix direction transverse shear failure ( $\sigma_4 > X_4$ ), fiber direction compressive failure ( $\sigma_{1C} > X_{1C}$ ), or matrix direction compressive failure ( $\sigma_{2C} > X_{2C}$ ). On the other hand, the dependent failure criterion adopted in the failure analysis is the Tsai-Hill criterion that states that failure occurs when the failure index  $D$  is equal to or greater than 1:

$$D \geq 1 \quad (2a)$$

with

$$D = (\sigma_1 / X_1)^2 + (\sigma_2 / Y)^2 - \sigma_1 \sigma_2 [(1 / X^2) + (1 / Y^2)] + (\sigma_4 / X_4)^2 + (\sigma_5 / X_5)^2 + (\sigma_6 / X_6)^2 \quad (2b)$$

Received 23 April 1998; revision received 3 May 1999; accepted for publication 4 May 1999. Copyright © 1999 by the American Institute of Aeronautics and Astronautics, Inc. All rights reserved.

\*Professor, Mechanical Engineering Department. Member AIAA.

†Graduate Student, Mechanical Engineering Department.

The values of  $X$  and  $Y$  are taken either as  $X_1$  and  $X_2$  or as  $X_{1C}$  and  $X_{2C}$ , depending on the sign of  $\sigma_1$  and  $\sigma_2$ , respectively.

### Reliability Analysis

The reliability model used for analyzing a laminated composite plate composed of  $NL$  layers is formulated on the basis of the following assumptions: 1) The constituent laminas of the composite laminate possess the same material properties and distributions of strength parameters. 2) Except strength parameters, other material constants are assumed to be deterministic in the reliability analysis. 3) The strength parameters are treated as independent baseline random variables. 4) Failure can only initiate at some critical points in a lamina, and the failure probabilities of those points are used to determine the failure probability of the lamina. 5) The laminated composite plate is modeled as a series system that is composed of  $NL$  components. 6) The lamina failure probabilities are treated as the component failure probabilities of the series system. Hence, in view of these assumptions, the system reliability of the laminated composite plate is expressed as

$$P_S = \prod_{j=1}^{NL} (1 - P_{fj}) \quad (3)$$

where  $\Pi$  is the notation of multiplication,  $P_S$  is system reliability, and  $P_{fj}$  is component failure probability. The method used for determining component (lamina) failure probability depends on the type of failure criterion adopted in the failure analysis of the laminated composite plate and is described as follows.

#### Independent (Stress) Criterion

In the probabilistic failure analysis, the largest values of the stress components, which may not occur at the same point, in each lamina of the plate are identified in the finite element analysis and are observed in the maximum stress criterion of Eq. (1). Any of the largest stress components in the lamina that satisfies the maximum stress criterion will lead to the failure of the lamina. The failure probability induced by the  $i$ th maximum stress component in the  $j$ th lamina is written as

$$P_{fij} = 1 - \prod_{k=1}^{NP} P[X_i \geq \sigma_{i|j}]_k \quad (4)$$

where  $P_{fij}$  is the component failure probability of the  $j$ th lamina due to the  $i$ th maximum stress component,  $P[\cdot]$  is the probability of the event in the brackets,  $\sigma_{i|j}$  is the largest value of the  $i$ th stress component in the  $j$ th lamina, and  $NP$  is the number of points at which stress components  $\sigma_{i|j}$  are the same. If the probability density function of  $X_i$  is  $f_{X_i}(x_i)$ , Eq. (4) can be rewritten as

$$P_{fij} = 1 - \prod_{k=1}^{NP} \left[ \int_{\sigma_{i|j}}^{\infty} f_{X_i}(x_i) dx_i \right]_k \quad (5)$$

The preceding integration can be solved analytically or numerically depending on the form of  $f_{X_i}(x_i)$ . The component failure probability of the  $j$ th lamina can then be expressed as

$$P_{fj} = 1 - \prod_{i=1, i \neq 3}^6 (1 - P_{fij}) \quad (6)$$

#### Dependent (Tsai-Hill) Failure Criterion

In this reliability model, the critical points, where their failure indices possess the largest value, in each lamina are determined from the deterministic failure analysis of the laminated composite plate, and their failure probabilities are used to compute the lamina failure probability. Note that the number of critical points in a lamina depends on the type of loading that is acting on the laminated plate. For instance, for a centrally loaded square plate, there is only one critical point in each lamina. In view of Eq. (2), the limit state equation for any of the critical points in a lamina is written as

$$1 - D = 0 \quad (7)$$

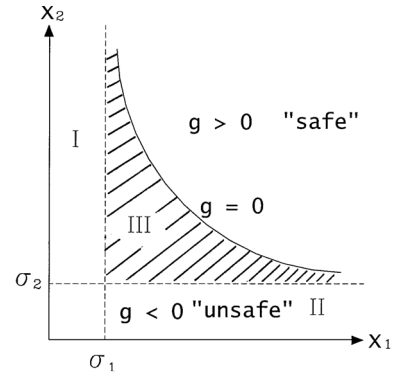


**Fig. 1** Limit state curve for the case with two random strength parameters.

For simplicity, the preceding limit state equation is rewritten as

$$g(x_1, \dots, x_k) = 0 \quad (8)$$

where the subscript  $k$  is the number of random parameters.

The failure probability of this limit state at the  $i$ th critical point of the  $j$ th lamina is expressed as

$$P_{fij} = \int_{g_{ij} < 0} \dots \int f_{X_1}(x_1) \dots f_{X_k}(x_k) dx_1 \dots dx_k \quad (9)$$

where the subscripts  $i$  and  $j$  are the  $i$ th critical point and  $j$ th lamina, respectively. The evaluation of the failure probability of Eq. (9) will be accomplished using a direct numerical integration method. The two-dimensional problem of Eq. (8) is used as an example to illustrate the present method. Figure 1 shows the shape of the limit state equation, which is defined as the failure curve, in the strength space comprising two random strength parameters  $X_1$  and  $X_2$ . The failure curve divides the strength space into safe and unsafe regions. The unsafe region is further divided into three subregions (I, II, and III) as shown in Fig. 1. According to the axiom of probability of union, the failure probability can be expressed as the sum of the probabilities over the subregions:

$$P_{fij} = \tilde{P}_{f_2} + \tilde{P}_{f_1} + \tilde{P}_{f_{02}} - P_f^* \quad (10)$$

with

$$\tilde{P}_{f_2} = \int_0^{\infty} \int_0^{\sigma_2} f_{X_1}(x_1) f_{X_2}(x_2) dx_1 dx_2 \quad (11a)$$

$$\tilde{P}_{f_1} = \int_0^{\infty} \int_0^{\sigma_1} f_{X_1}(x_1) f_{X_2}(x_2) dx_1 dx_2 \quad (11b)$$

$$P_f^* = \int_0^{\sigma_1} \int_0^{\sigma_2} f_{X_1}(x_1) f_{X_2}(x_2) dx_1 dx_2 \quad (11c)$$

$$\tilde{P}_{f_{02}} = \int_{\sigma_1}^{\infty} \int_{\sigma_2}^{X'_2} f_{X_1}(x_1) f_{X_2}(x_2) dx_1 dx_2 \quad (11d)$$

where  $X'_2$  is determined from the solution of the limit state equation  $g = 0$  and  $P_f^*$  is the probability over the area of intersection between subregions I and II. In view of the theorem of marginal probability, Eqs. (11a) and (11b) can be simplified as

$$\tilde{P}_{f_1} = \int_0^{\sigma_1} f_{X_1}(x_1) dx_1 \quad (12a)$$

$$\tilde{P}_{f_2} = \int_0^{\sigma_2} f_{X_2}(x_2) dx_2 \quad (12b)$$

The preceding integrations can be easily solved analytically or numerically. In view of Eq. (12), Eq. (11c) can be rewritten as

$$P_f^* = \tilde{P}_{f_1} \cdot \tilde{P}_{f_2} \quad (13)$$

The probability of Eq. (11d), which is the probability over subregion III (shaded area) in Fig. 1, will be approximated as

$$\tilde{P}_{f02} \cong \int_{\sigma_1}^{x_{\max}} \int_{\sigma_2}^{x_2'} f_{X_1}(x_1) f_{X_2}(x_2) dx_1 dx_2 \tag{14}$$

where  $x_{\max}$  is a sufficiently large number beyond which the joint probability of  $x_1$  and  $x_2$  is too small to be considered. In numerical integration form, Eq. (14) is written as

$$\tilde{P}_{f02} = \sum_{i=1}^{NQ} W_i \left[ \sum_{j=1}^{NR} C_{ij} f_{X_1}(x_{1i}) f_{X_2}(x_{2j}) \right] \tag{15}$$

where  $W_i$  and  $C_{ij}$  are weighting factors,  $NQ$  and  $NR$  are the numbers of integration points, and  $x_{1i}$  and  $x_{2j}$  are coordinates of integration points in the  $X_1$  and  $X_2$  directions, respectively. The foregoing procedure can be easily extended to cases containing  $n$  random strength parameters via the repeated use of the axiom of probability of union. A recursive equation for the case of  $n$  random variables is, thus, expressed as

$$P_{fij} = P_n + \tilde{P}_{f0n} \tag{16a}$$

with

$$P_k = P_{k-1} + \tilde{P}_{fk} - P_{k-1} \cdot \tilde{P}_{fk}, \quad k = 2, 3, \dots, n \tag{16b}$$

$$\tilde{P}_{fn} = \int_0^{\sigma_n} f_{X_n}(x_n) dx_n \tag{16c}$$

$$\tilde{P}_{f0n} = \int_{\sigma_1}^{\infty} \cdots \int_{\sigma_{n-1}}^{\infty} \int_{\sigma_n}^{x_n'} f_{X_1}(x_1) \cdots f_{X_n}(x_n) dx_1 \cdots dx_n \tag{16d}$$

where  $x_n'$  is determined by satisfying the limit state equation, that is,  $g(x_1, \dots, x_{n-1}, x_n') = 0$ .

In particular, the failure probabilities for the cases of  $n = 3$  and 6 are determined from the following equations.

Case  $n = 3$ :

$$P_{fij} = P_3 + \tilde{P}_{f03} \tag{17a}$$

with

$$P_3 = P_2 + \tilde{P}_{f3} - P_2 \cdot \tilde{P}_{f3} \tag{17b}$$

$$P_2 = \tilde{P}_{f1} + \tilde{P}_{f2} - \tilde{P}_{f1} \cdot \tilde{P}_{f2} \tag{17c}$$

Case  $n = 6$ :

$$P_{fij} = P_6 + \tilde{P}_{f06} \tag{18a}$$

with

$$P_6 = P_5 + \tilde{P}_{f6} - P_5 \cdot \tilde{P}_{f6} \tag{18b}$$

$$P_5 = P_4 + \tilde{P}_{f5} - P_4 \cdot \tilde{P}_{f5} \tag{18c}$$

$$P_4 = P_3 + \tilde{P}_{f4} - P_3 \cdot \tilde{P}_{f4} \tag{18d}$$

The accuracy of the numerical integration technique used in evaluating Eqs. (17) and (18) has been verified by the Monte Carlo method in which over 5000 trials were generated, and the differences between the results obtained by the present method and those by the Monte Carlo method are negligible. Based on the weakest link hypothesis, the lamina failure probability is then obtained as

$$P_{fj} = 1 - \prod_{i=1}^{NC} (1 - P_{fij}) \tag{19}$$

where  $NC$  is the number of critical points in a lamina.

Experimental Investigation

Tests of centrally loaded square laminated composite plates of length  $a = 100$  and 50 mm and ply thickness  $h_i = 0.121$  mm were

Table 1 Material properties of graphite/epoxy lamina

Material constant	Value
$E_1$	139.4 GPa
$E_2$	7.65 GPa
$G_{12} = G_{13}$	4.35 GPa
$G_{23}$	1.02 GPa
$\nu_{12}$	0.29

Table 2 Statistics of strength parameters

Strength parameter	Mean value, MPa	COV, %	Weibull distribution	
			Shape parameter	Scale parameter, MPa
$X_1 = X_T$	1537.2	2.1	46.67	1553.73
$X_2 = Y_T$	44.44	4.2	27.41	45.26
$X_4 = R$	79.67	5.7	17.51	81.92
$X_5 = S$	102.42	5.7	22.50	105.26
$X_6 = S$	102.42	5.7	22.50	105.26
$X_{1C} = X_C$	1722.1	2.1	52.28	1740.84
$X_{2C} = Y_C$	213.95	6.3	81.80	220.33

performed to study the probability distribution of first-ply failure load for the plates. The laminated composite plates under consideration were made of graphite/epoxy (Q-1115) prepreg tapes supplied by the Toho Company, Japan. The material properties were determined from experiments conducted in accordance with the relevant American Standards for Testing and Materials standards,<sup>11</sup> and their mean values are given in Table 1. The statistics of each lamina strength parameter was determined from a set of 17 specimens. The strength parameter data were fitted by the Weibull distribution using the Weibull probability paper. Figure 2 shows the experimentally determined Weibull density function of  $X_2$  in comparison with the histogram of the strength parameter. It has been found that in general the experimental data of all of the strength parameters can be well fitted by the Weibull distribution. Table 2 lists the statistics of the strength parameters. The experimental apparatus for first-ply failure tests consisted of a 10-ton Instron testing machine, an acoustic emission (AE) system (AMSY4) with two AE sensors, a data acquisition system, a steel load applicator with a spherical head of radius  $r = 5$  mm, and a fixture for clamping a specimen. The AMSY4 system was developed and manufactured by Vallen Systeme GmbH, Munich, Germany. The fixture was made of two square steel frames. During testing, the laminated plate was clamped by the two steel frames, which were connected together by four bolts. It is noted that the clamping method allowed no rotations at the edges of the laminated plate during loading. A stroke control approach was adopted in constructing the load-deflection relation for the laminated plate. The loading rate was slow enough for inertia effects to be neglected. During loading, two AE sensors were used to measure the stress waves released at the AE sources in the laminated plate. The measured AEs were converted by the AMSY4 (AE) system to a set of signal parameters, such as peak amplitude, energy, rise time, and duration, which were then used to identify the first-ply failure load of the laminated plate. Detailed description of the experimental setup and the identification method may be found in the literature.<sup>12,13</sup> A set of 19–22 specimens for each layout and plate size was subjected to the first-ply failure testing. Again, the experimental first-ply failure load data were well curve fitted by the Weibull distribution. For instance, Figs. 3 and 4 show the experimental first-ply failure load data of the 50 × 50 mm [0<sub>6</sub>/90<sub>6</sub>]<sub>s</sub>-deg plates and 100 × 100 mm [45/−45<sub>2</sub>/45<sub>9</sub>]<sub>s</sub>-deg plates respectively, fitted by the Weibull distribution. The statistics of the first-ply failure loads for the laminated composite plates are listed in Table 3. In general the variations of the first-ply failure loads of the laminated plates are small [coefficient of variation (COV) less than 7%], and the mean first-ply failure load decreases as the size of the plates reduces. Visual inspection of the failed specimens was performed. A large matrix crack was always observed at the center of the bottom surface of each specimen.

Table 3 Statistics of first-ply failure load for different laminated composite plates

Layup, deg	First-ply failure load							
	<i>a</i> = 50 mm				<i>a</i> = 100 mm			
	Mean, MPa	COV, %	Weibull distribution		Mean, MPa	COV, %	Weibull distribution	
			Shape parameter	Scale parameter			Shape parameter	Scale parameter
[0/90 <sub>2</sub> /0 <sub>9</sub> ] <sub>s</sub>	—	—	—	—	1841.1	4.69	25.19	1878.14
[0 <sub>6</sub> /90 <sub>6</sub> ] <sub>s</sub>	1124.98	4.99	23.782	1148.75	1218.9	5.95	18.97	1250.87
[45/−45 <sub>2</sub> /45 <sub>9</sub> ] <sub>s</sub>	—	—	—	—	2092.6	6.47	18.49	2148.21
[45 <sub>6</sub> /−45 <sub>6</sub> ] <sub>s</sub>	1243.19	5.36	11.31	1294.95	1296.9	6.40	18.39	1331.58

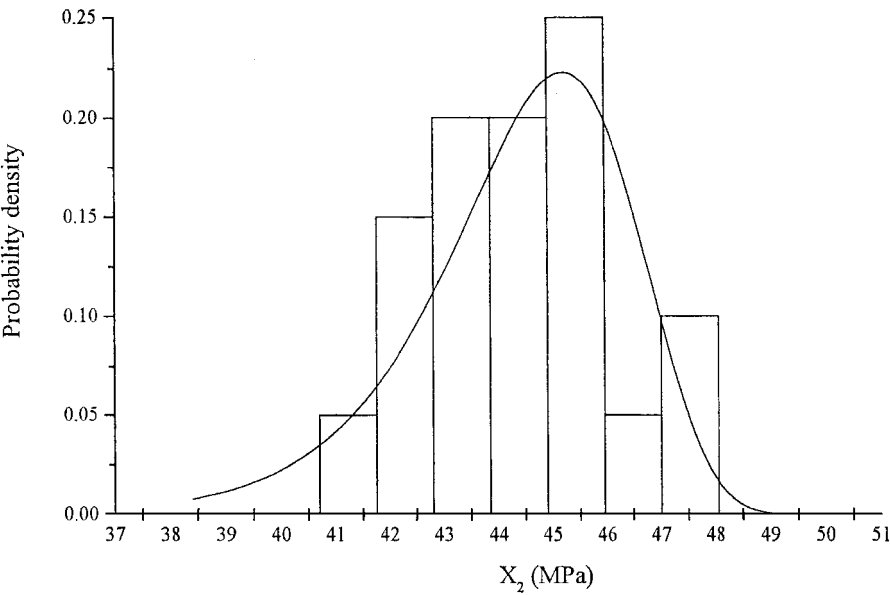


Fig. 2 Histogram of strength parameter in matrix direction ( $X_2$ ) fitted by Weibull distribution.

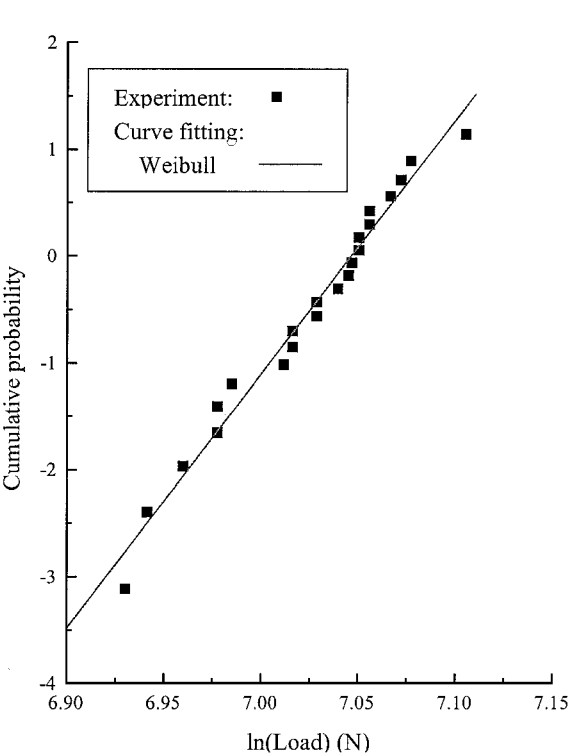


Fig. 3 Experimental first-ply failure load data of the  $[0_6/90_6]_s$ -deg plate fitted by Weibull distribution ( $a = 50$  mm).

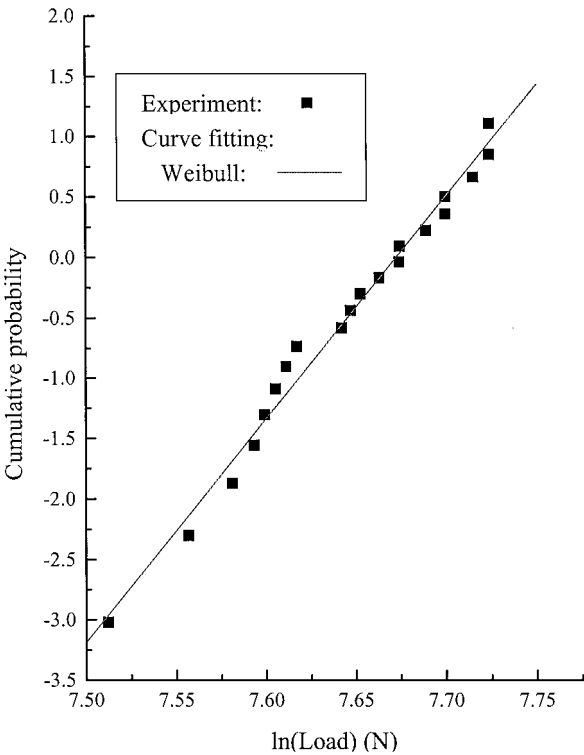


Fig. 4 Experimental first-ply failure load data of the  $[45/-45_2/45_9]_s$ -deg plate fitted by Weibull distribution ( $a = 100$  mm).

Table 4 Failure probabilities of laminated composite plates obtained using different methods ( $a = 100\text{ mm}$ )

Layup, deg	$P, N$	Most critical point			Plate failure probability		Difference, %	
		Stress	Failure probability		Theoretical (II)	Experimental (III)	$\frac{\text{III} - \text{I}}{\text{III}}$	$\frac{\text{III} - \text{II}}{\text{III}}$
			Component	Total (I)				
$[0_6/90_6]_s$	1250	$\sigma_1$	$1.018 \times 10^{-28}$	$6.052 \times 10^{-1}$	$6.425 \times 10^{-1}$	$6.273 \times 10^{-1}$	3.523	-2.423
		$\sigma_2$	$6.052 \times 10^{-1}$					
		$\sigma_4$	$7.585 \times 10^{-21}$					
		$\sigma_5$	$7.967 \times 10^{-12}$					
		$\sigma_6$	$1.920 \times 10^{-28}$					
$[45/-45_2/45_9]_s$	2160	$\sigma_1$	$2.735 \times 10^{-20}$	$6.373 \times 10^{-1}$	$6.810 \times 10^{-1}$	$6.693 \times 10^{-1}$	4.781	-1.748
		$\sigma_2$	$6.373 \times 10^{-1}$					
		$\sigma_4$	$7.296 \times 10^{-13}$					
		$\sigma_5$	$1.840 \times 10^{-33}$					
		$\sigma_6$	$2.889 \times 10^{-35}$					
$[0/90_2/0_9]_s$	1900	$\sigma_1$	$2.613 \times 10^{-20}$	$6.906 \times 10^{-1}$	$7.453 \times 10^{-1}$	$7.377 \times 10^{-1}$	6.385	-1.030
		$\sigma_2$	$6.906 \times 10^{-1}$					
		$\sigma_4$	$3.522 \times 10^{-13}$					
		$\sigma_5$	$2.749 \times 10^{-11}$					
		$\sigma_6$	$1.993 \times 10^{-21}$					
$[45_6/-45_6]_s$	1330	$\sigma_1$	$8.501 \times 10^{-30}$	$5.900 \times 10^{-1}$	$6.275 \times 10^{-1}$	$6.241 \times 10^{-1}$	5.464	-0.545
		$\sigma_2$	$5.900 \times 10^{-1}$					
		$\sigma_4$	$5.724 \times 10^{-18}$					
		$\sigma_5$	$2.004 \times 10^{-35}$					
		$\sigma_6$	$1.060 \times 10^{-40}$					

Examples and Discussion

The reliability of a number of clamped and centrally loaded laminated composite plates of different lamination arrangements, namely,  $[0_6/90_6]_s$ ,  $[0/90_2/0_9]_s$ ,  $[45_6/-45_6]_s$ , and  $[45/-45_2/45_9]_s$  deg is studied. The material properties of the composite laminates are listed in Table 1. The ability of the aforementioned finite element method in predicting accurate mechanical behaviors of laminated composite plates has been verified by the experimental results reported in the literature.<sup>13, 14</sup> In the finite element analysis, it has been found that the use of a  $6 \times 6$  mesh over the full plate for the  $[45_6/-45_6]_s$ - and  $[45/-45_2/45_9]_s$ -deg plates can yield displacements in better agreement with the experimental results. On the other hand, for the orthotropically laminated composite  $[0_6/90_6]_s$ - and  $[0/90_2/0_9]_s$ -deg plates, the use of a  $4 \times 4$  mesh over a quarter plate is enough to yield good results. The finite element meshes adopted in the displacement analysis can also yield reasonably accurate stresses in the plates, as will be demonstrated in the following. Note that there is a stress singularity at the center of a centrally loaded plate, and thus a finer finite element mesh produces higher stresses in the plate. Now consider the failure mode and reliability analyses of the laminated composite plates subjected to a centerpoint load with different magnitudes. In the deterministic failure analyses of the laminated composite plates, the most critical points are identified to be at the center of the bottom surfaces of the plates. Based on the maximum stress criterion and the statistics of the strength parameters in Table 2, the system reliability and the component failure probabilities at the most critical points of the laminated composite plates ( $a = 100\text{ mm}$ ) are computed using Eqs. (3) and (4), respectively, and the results are listed in Table 4 in comparison with the experimental system failure probabilities that are determined from the experimental distributions. Note that the dominant failure modes of the plates, which are manifested by the largest component failure probabilities listed in Table 4, are matrix tension fracture, and this has also been confirmed by the visual inspection of the specimens that have been tested. Except  $Y_T$ , the contributions of the uncertainties of other strength parameters to the failure probabilities of the laminated plates are insignificant and, thus, negligible. Also note that, as indicated by the signs ahead of the differences in Table 4, the mere consideration of the failure probability of the most critical point of a laminated plate underestimates the system failure probability of the plate (difference is positive), whereas the consideration of the failure probabilities of all of the laminas slightly overestimates the system failure probability of the plate (difference is negative). The small differences between the theoretical (considering all layer failure probabilities) and experimental system failure probabilities,

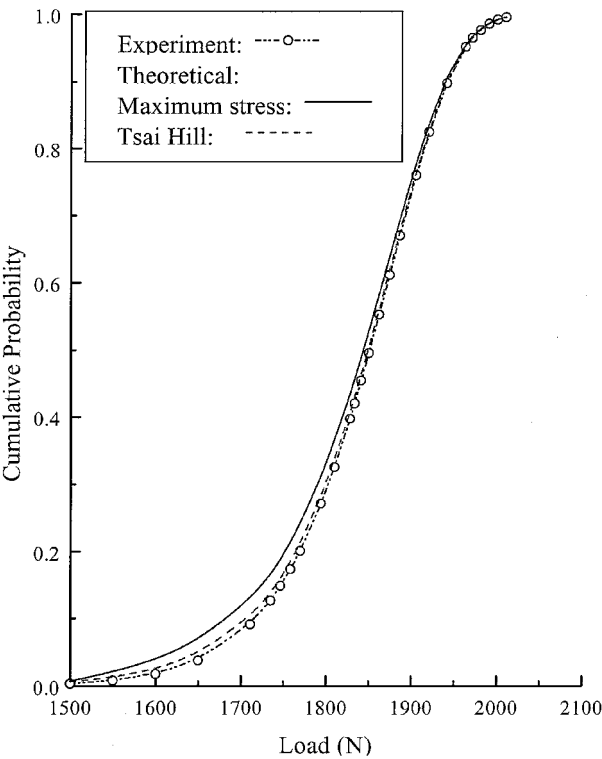


Fig. 5 Experimental and theoretical probability distributions of the first-ply failure load of the  $[0/90_2/0_9]_s$ -deg plate with  $a = 100\text{ mm}$ .

which are less than 7%, verify the suitability and accuracy of the present reliability model. Next, the effects of the type of failure criterion on reliability of laminated composite plates are studied. The failure criteria, namely, maximum stress (independent) and Tsai-Hill (dependent) failure criteria, are used in turn in the reliability analysis of the laminated composite plates with different sizes. The theoretically predicted system failure probabilities of the plates are compared with the experimentally determined Weibull distributions, as shown in Figs. 5–10. Note that both failure criteria can produce very good results irrespective of plate size. The overall good agreements between the theoretical and experimental system failure probability

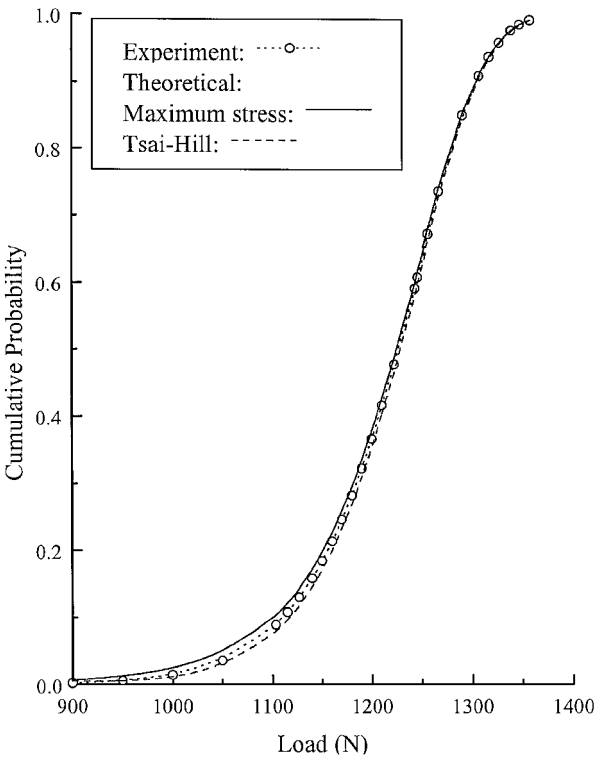


Fig. 6 Experimental and theoretical probability distributions of the first-ply failure load of the  $[0_6/90_6]_s$ -deg plate with  $a = 100$  mm.

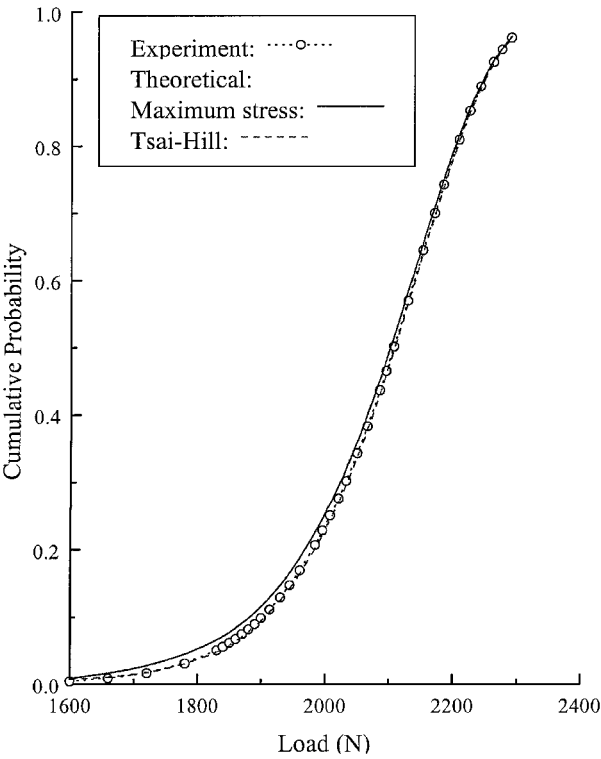


Fig. 8 Experimental and theoretical probability distributions of the first-ply failure load of the  $[45/-45_2/45_9]_s$ -deg plate with  $a = 100$  mm.

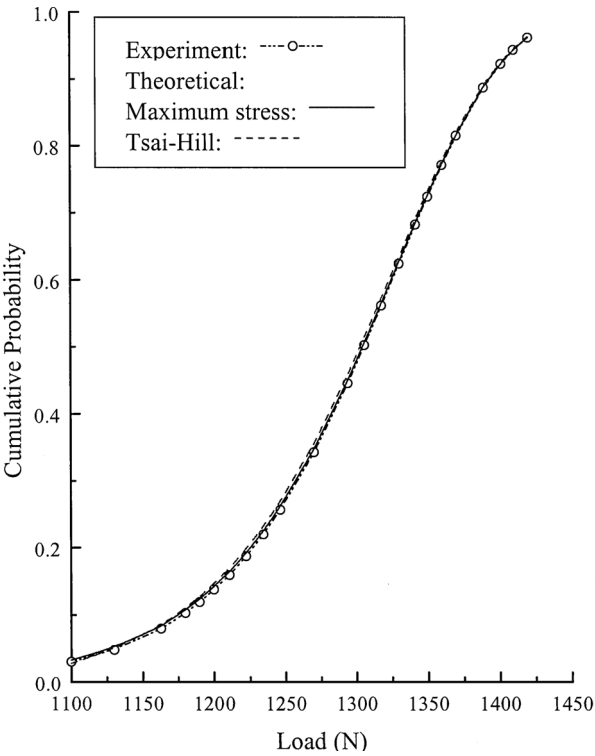


Fig. 7 Experimental and theoretical probability distributions of the first-ply failure load of the  $[45_6/-45_6]_s$ -deg plate with  $a = 100$  mm.

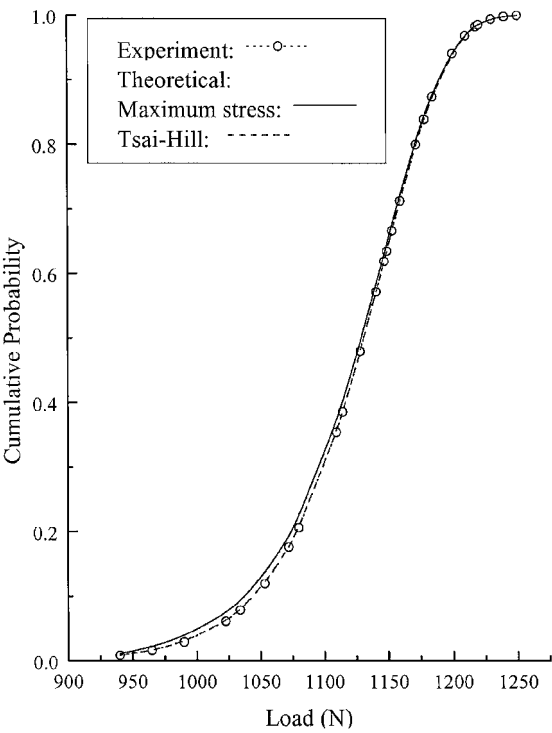


Fig. 9 Experimental and theoretical probability distributions of the first-ply failure load of the  $[0_6/90_6]_s$ -deg plate with  $a = 50$  mm.

distributions for the plates further demonstrate the suitability of the present method. Note that for real structures the failure probabilities of the structures are usually small. Therefore, it is required to have an appropriate reliability method capable of predicting the small failure probability for the structures. In Figs. 5–10, for  $P_f < 0.1$ , that is, at the lower tails of the distributions, close agreements between the theoretical and experimental distributions of system failure probability can be obtained for the laminated composite plates. For further comparison, some typical reliabilities of the plates subjected to a centerpoint load with different magnitudes are listed in

Table 5 for comparison. The comparison between the theoretical and experimental reliabilities shows that the present method can predict accurate reliabilities for the laminated composite plates with overall error less than 6% irrespective of plate size or the type of failure criterion adopted in the reliability analysis. The negative sign ahead of any of the differences means that the theoretical reliability is larger than the experimental one. It is also worth noting that the reliability of the laminated composite plates increases as the sizes of the plates increase. For instance, when subjected to  $P = 1100$  N, the reliability of the  $[45_6/-45_6]_s$ -deg plate increases from 0.85390 to 0.97006 as the plate size increases from  $50 \times 50$  to  $100 \times 100$  mm.

Table 5 Reliability of laminated composite plates with different sizes predicted by various methods

Layup, deg	a, mm	Load, N	Plate reliability			Difference, %	
			Theoretical		Experimental (III)	$\frac{III - I}{III} \times 100$	$\frac{III - II}{III} \times 100$
			Maximum stress (I)	Tsai-Hill (II)			
[0/90 <sub>2</sub> /0 <sub>9</sub> ] <sub>s</sub>	100	1500	0.99290	0.99432	0.99653	0.364	0.221
		1800	0.66877	0.69722	0.70888	5.66	1.64
[0 <sub>6</sub> /90 <sub>6</sub> ] <sub>s</sub>		900	0.99392	0.99518	0.99806	0.415	0.288
		1200	0.62267	0.64722	0.63445	1.86	-2.01
[45/-45 <sub>2</sub> /45 <sub>9</sub> ] <sub>s</sub>		1600	0.99120	0.99286	0.99570	0.452	0.284
		2000	0.74738	0.77154	0.76587	2.42	-0.74
[45 <sub>6</sub> /-45 <sub>6</sub> ] <sub>s</sub>		1100	0.96732	0.97244	0.97006	0.282	-0.245
		1175	0.90399	0.91581	0.90470	0.08	-1.23
[0 <sub>6</sub> /90 <sub>6</sub> ] <sub>s</sub>	50	940	0.98913	0.99180	0.99155	0.244	-0.025
		1050	0.87258	0.88736	0.88800	1.73	0.07
[45 <sub>6</sub> /-45 <sub>6</sub> ] <sub>s</sub>		900	0.98427	0.98714	0.98380	-0.048	-0.339
		1100	0.84524	0.86193	0.85390	1.01	-0.94

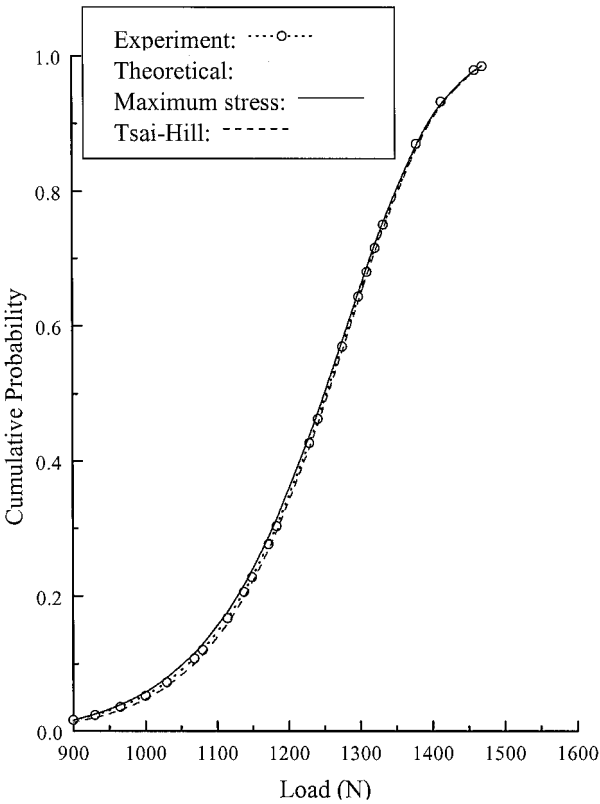


Fig. 10 Experimental and theoretical probability distributions of the first-ply failure load of the [45<sub>6</sub>/-45<sub>6</sub>]<sub>s</sub>-deg plate with a = 50 mm.

This phenomenon is mainly because a decrease in plate size raises the stress magnitudes, which can, thus, reduce the mean first-ply failure load and, consequently, the reliability of the plate as having been manifested in Tables 3 and 5, respectively.

In this study, the applications of the present method have been demonstrated by means of a number of examples. The present method could produce reliabilities with sufficient accuracy for the laminated composite plates even though only strength parameters were treated as baseline random variables. In some cases, however, the randomness of other parameters, such as material characteristics, ply angle, layer thickness, etc., may also play a significant role on the reliability predictions of composite structures.<sup>15</sup> Thus, it will be more appropriate if all random parameters are considered in the reliability analysis of composite structures. In fact, with some modifications, the inclusion of all random parameters in the present method can be achieved, and this will be reported in a forthcoming paper.

Conclusions

A method constructed on the basis of a phenomenological failure criterion and the series system hypothesis was presented for the reliability assessment of laminated composite plates subjected to transverse loads. The independent(maximum stress) and dependent quadratic(Tsai-Hill) failure criteria were adopted in formulating the reliability models, and numerical techniques were presented for reliability evaluation in the reliability study of the laminated composite plates. Experiments were performed to study the distributions of lamina strength parameters and first-ply failure load of laminated composite plates. It was shown that the experimental data were well fitted by the Weibull distribution. The accuracy of the present method in reliability prediction was verified against the experimental results. In general, the present method could yield very accurate results for the plates irrespective of which type of failure criterion was adopted in the reliability analysis. The failure mode as well as the strength parameters that have important effects on the reliability of the laminated composite plates were studied. The dominant failure mode of the centrally loaded plates was matrix tension cracking. Among the strength parameters, the randomness of the tensile strength in the matrix direction  $Y_T$  had the most significant effect on the reliability of the plates. The failure of the most critical point in any of the laminated composite plates had the major contribution to the failure probability of the plate. The size effects on the reliability of the laminated composite plates were also studied. It was found that when subjected to a centerpoint load, the reliability of the laminated plates increased as the sizes of the plates increased. This phenomenon was attributed to the decrease in stress magnitudes and the increase in mean first-ply failure load as plate size increased.

Acknowledgment

This research was supported in part by the National Science Council under Grant NSC 86-2623-D009-008.

References

<sup>1</sup>Cederbaum, G., Elishakoff, I., and Librescu, L., "Reliability of Laminated Plates via the First-Order Second Moment Method," *Journal of Composite Structures*, Vol. 15, No. 2, 1990, pp. 161-167.  
<sup>2</sup>Cederbaum, G., and Aboudi, J., "Reliability of Composites Based on Micromechanically Predicted Strength and Fatigue Criteria," *Composite Structures 6*, edited by I. H. Marshall, Elsevier, London, 1991, pp. 75-88.  
<sup>3</sup>Sun, C. T., and Yamada, S. E., "Strength Distribution of a Unidirectional Fiber Composite," *Journal of Composite Materials*, Vol. 12, April 1978, pp. 169-176.  
<sup>4</sup>Cassenti, B. N., "Probabilistic Static Failure of Composite Material," *AIAA Journal*, Vol. 22, No. 1, 1984, pp. 103-110.  
<sup>5</sup>Gurvich, M. R., and Pipes, R. B., "Probabilistic Analysis of Multi-Step Failure Process of a Laminated Composite in Bending," *Composites Science and Technology*, Vol. 55, No. 4, 1995, pp. 413-421.  
<sup>6</sup>Kam, T. Y., and Lin, S. C., "Reliability Analysis of Laminated Composite Plates," *Proceedings of the National Science Council of the Republic of China*, Pt. A, Vol. 16, No. 2, 1992, pp. 163-171.

<sup>7</sup>Kam, T. Y., Lin, S. C., and Hsiao, K. M., "Reliability Analysis of Non-linear Laminated Composite Plate Structures," *Journal of Composite Structures*, Vol. 25, Nos. 1-4, 1993, pp. 503-510.

<sup>8</sup>Engelstad, S. P., and Reddy, J. N., "Probabilistic Nonlinear Finite Element Analysis of Composite Structures," *AIAA Journal*, Vol. 31, No. 2, 1993, pp. 362-369.

<sup>9</sup>Kam, T. Y., and Chang, R. R., "Finite Element Analysis of Shear Deformable Laminated Composite Plates," *Journal of Energy Resources Technology*, Vol. 115, March 1993, pp. 41-46.

<sup>10</sup>Tsai, S. W., and Hahn, H. T., *Introduction to Composite Materials*, Technomic, Westport, CT, 1980, Chap. 7.

<sup>11</sup>*Standards and Literature References for Composite Material*, 2nd ed., American Society for Testing and Materials, Philadelphia, 1990.

<sup>12</sup>Kam, T. Y., Sher, H. F., Chao, T. N., and Chang, R. R., "Predictions of Deflection and First-Ply Failure Load of Thin Laminated Composite Plates

via the Finite Element Approach," *Journal of Solids and Structures*, Vol. 33, No. 3, 1996, pp. 375-398.

<sup>13</sup>Kam, T. Y., and Lai, F. M., "Experimental and Theoretical Predictions of First-Ply Failure Strength of Laminated Composite Plates," *Journal of Solids and Structures*, Vol. 36, No. 16, 1999, pp. 2379-2395.

<sup>14</sup>Chu, K. H., "Reliability Analysis of Laminated Composite Components," Ph.D. Dissertation, Mechanical Engineering Dept., National Chiao Tung Univ., Hsin-Chu, Taiwan, ROC, 1998.

<sup>15</sup>Oh, D. H., and Librescu, L., "Free Vibration and Reliability of Composite Cantilevers Featuring Uncertain Properties," *Reliability Engineering and System Safety*, Vol. 56, No. 3, 1997, pp. 265-272.

G. A. Kardomateas  
Associate Editor